Intravenous Followed by X-ray Fused with MRI-Guided Transendocardial Mesenchymal Stem Cell Injection Improves Contractility Reserve in a Swine Model of Myocardial Infarction

Eric G. Schmuck[1], **Jill M. Koch**[1], **Timothy A. Hacker**[1], **Charles R. Hatt**[2], **Michael T. Tomkowiak**[2], **Karl K. Vigen**[3], **Nicholas Hendren**[1], **Cathlyn Leitzke**[1], **Ying-qi Zhao**[4], **Zhanhai Li**[4], **John M. Centanni**[1], **Derek J. Hei**[5], **Denise Schwahn**[6], **Jaehyup Kim**[7], **Peiman Hematti**[7], and **Amish N. Raval**[1,2]

Amish N. Raval: anr@medicine.wisc.edu

[1]Division of Cardiovascular Medicine, Department of Medicine, University of Wisconsin School of Medicine and Public Health, Madison, WI, USA

[2]Division of Cardiovascular Medicine, Department of Biomedical Engineering, University of Wisconsin School of Medicine and Public Health, H4/568 Clinical Sciences Center, 600 Highland Ave, Madison, WI 53792-3248, USA

[3]Division of Radiology, Department of Medicine, University of Wisconsin School of Medicine and Public Health, Madison, WI, USA

[4]Department of Biostatistics and Medical Informatics, University of Wisconsin School of Medicine and Public Health, Madison, WI, USA

[5]Waisman Biomanufacturing Facility, Madison, WI, USA

[6]Research Animal Resources Center, University of Wisconsin, Madison, WI, USA

[7]Division of Hematology/Oncology, Department of Medicine, University of Wisconsin School of Medicine and Public Health, Madison, WI, USA

Abstract

The aim of this study is to determine the effects of early intravenous (IV) infusion later followed by transendocardial (TE) injection of allogeneic mesenchymal stem cells (MSCs) following myocardial infarction (MI). Twenty-four swine underwent balloon occlusion reperfusion MI and were randomized into 4 groups: IV MSC (or placebo) infusion (post-MI day 2) and TE MSC (or placebo) injection targeting the infarct border with 2D X-ray fluoroscopy fused to 3D magnetic resonance (XFM) co-registration (post-MI day 14). Continuous ECG recording, MRI, and invasive pressure-volume analyses were performed. IV MSC plus TE MSC treated group was superior to

other groups for contractility reserve (p=0.02) and freedom from VT (p=0.03) but had more lymphocytic foci localized to the peri-infarct region (p= 0.002). No differences were observed in post-MI remodeling parameters. IV followed by XFM targeted TE MSC therapy improves contractility reserve and suppresses VT but does not affect post-MI remodeling and may cause an immune response.

Keywords

Mesenchymal stem cell; Transendocardial; Intravenous; Swine; Stem cell; Allogeneic; Myocardial infarction; Multiple dose; Immune response

Introduction

Myocardial infarction (MI) is a common and deadly condition that is characterized by an acute inflammatory response to ischemia followed by outwardly expanding myocardial necrosis, left ventricular dilatation, increased left ventricular stiffness, and reduced contractile performance [1, 2]. Patients who present late or fail conventional therapies are at risk for developing heart failure and have a poor prognosis [3]. Stem cells have emerged as a promising approach to prevent post-MI pathological remodeling; however, the optimal cell type, delivery method, and dosing strategy remain unknown [4].

Mesenchymal stem cells (MSCs) are multi-potent progenitor cells with pro-angiogenic, and immune-modulatory properties [5–8]. They can be isolated from multiple sources, such as bone marrow, adipose, and cardiac tissue [9, 10], and expanded to large quantities and banked with relative ease. MSCs appear to be immunoprivileged due to the low expression of MHC class II, monocytic, or B cell markers [11]. Several groups have suggested that transplanted MSCs do not elicit a detectable allogeneic immune response, even in highly inflammatory environments and after serial dosing [12–16], although this property remains controversial. The totality of the evidence to date would suggest that MSCs are an ideal "off-the-shelf" therapy to curb post-MI pathological remodeling.

In early phase clinical trials involving recent MI, single dose intravenous or intracoronary infusion of various cell types has yielded mixed results with no trials reporting substantial long-term improvement [17–21]. Two suggestions have emerged from this experience: (i) MSC re-dosing may be required for sustained and/or amplified benefit, and (ii) early delivery of MSCs may exert greater benefit to "prevent" adverse remodeling rather than to "reverse" adverse remodeling if MSCs are delivered late. Intravenous infusion of MSCs within a few days post-MI is appealing because it is safe, the timing coincides with cell homing factor expression [22–24], and an early anti-inflammatory effect may provide a more hospitable environment in the injured myocardium in preparation for a second dose [25]. However, local homing factor expression declines after 2 weeks, reducing the likelihood of IV infused cells trafficking to the heart. Thus, repeat intravenous infusion at that time is not likely to be effective. Alternatively, transendocardial catheter injection is a minimally invasive delivery method to directly inject cells into the myocardium, thereby circumventing the need for homing. Intravenous cell infusion may be preferred over transendocardial injection in the first week post-MI due to safety concerns of catheter-

associated cardiac perforation at a time when the injured myocardium is highly edematous and friable. Furthermore, from a clinical perspective, intravenous infusion may be preferred early post-MI because it is easy to administer at any institution. If there has been no functional myocardial recovery after 2 weeks, the patient could be referred to a larger hospital with the resources necessary for repeat dosing using a catheter-based transendocardial injection delivery method. With accurate X-ray fused with MRI co-registration (XFM), MSCs can be transendocardially delivered precisely into the infarct border where therapeutic effect may be the greatest [26]. Therefore, the rational for timing and delivery are rooted in both the biological healing process and the clinical applicability of the delivery methods. Thus, we tested the hypothesis that early intravenous infusion followed by later XFM guided "targeted" transendocardial catheter delivery of bone marrow-derived allogeneic MSCs improves contractility reserve and curbs adverse remodeling post-MI.

Methods

Study Design

All procedures were performed in accordance with a local Institutional Animal Care and Use Committee approved protocol. Following the creation of an antero-septal myocardial infarction, surviving animals were randomized by computer-generated block randomization into four treatment groups: (i) intravenous (IV) administration of 100 million allogeneic MSCs at day 2 post-MI, followed by transendocardial (TE) administration of 100 million allogeneic MSCs at day 14 post-MI (++); (ii) IV placebo followed by TE MSCs (−+); (iii) IV MSCs followed by TE placebo (+−); and (iv) IV placebo and TE placebo (−−) (Fig. 1). The Helix/Morph (Biocardia Inc. Santa Clara, CA) corkscrew-shaped catheter was used in combination with the U. Wisconsin XFM Co-Registration Interventional Imaging System [26]. Laboratory personnel involved with treatment, monitoring of the animals, and analysis of all endpoints were blinded to treatment assignment. Animals were sacrificed at day 55 post-MI and a board-certified veterinary pathologist (D.S.) in a Good Laboratory Practice compliant laboratory performed detailed histopathology.

Acute Myocardial Infarction Model (Day 0)

Closed chest antero-septal MI was induced in 36 female Yorkshire swine weighing 30 kg using methods previously described by our group [26, 27]. Briefly, animals were sedated with an intramuscular injection of Telazol 4–6 mg/kg and Xylazine 2 mg/kg and then intubated and mechanically ventilated with 1–3 % isoflurane. Transfemoral arterial access was obtained with a 6 F introducer sheath using either Seldinger technique or surgical cut-down. A coronary guide catheter was advanced under fluoroscopic guidance to the left coronary artery ostium. Over a coronary guide wire, an appropriately sized coronary balloon catheter was introduced into the proximal left anterior descending artery (LAD) just beyond the first diagonal artery. The balloon was inflated until flow was obstructed and maintained for 90 min with continuous ECG monitoring for ST elevation and intermittent test angiograms to confirm occlusion. Adjunctive medications included heparin (70 U/kg), lidocaine (1 mg/kg), amiodarone (300 mg), and metoprolol (2.5–5 mg) all delivered intravenously. External defibrillation (200 J) was performed as necessary. Animals were

continuously monitored by laboratory personnel during recovery and then transferred to in-house holding pens where they were monitored daily by a veterinary staff and survived for 55 days.

MSC Isolation and Expansion

Porcine mesenchymal stem cells were isolated from a bone marrow aspirate of a single male Yorkshire donor using previously described methods [28]. Briefly, bone marrow aspirate was obtained from the iliac crest, and mononuclear cells were isolated using density gradient separation method by Ficoll-Hypaque 1.073 (GE Healthcare, Piscataway, NJ, USA) and Leucosep tube (Greiner Bioone, Monroe, NC, USA) according to the manufacturer's protocol. Isolated mononuclear cells were treated with ACK buffer to lyse the RBCs and plated in alpha minimum essential media (aMEM) supplemented with 10 % fetal bovine serum (Hyclone, Logan, UT, USA), non-essential amino acids, and L-alanine-l-glutamine (Mediatech, Manassas, VA, USA). When cells reached 80–90 % confluency, they were harvested using TrypLE (Invitrogen, Carlsbad, CA, USA) and re-plated at 2000 cells/cm^2 density and expanded in MSC Complete Medium consisting of alpha-MEM (Mediatech, Manassas, VA) supplemented with 10 % FBS (Life Technologies, Grand Island, NY), 1× GlutaMax (Life Technologies), and 1 ng/mL FGF-2 (Waisman Biomanufacturing). A master cell bank (MCB) was generated at passage 2 (P2) and was frozen in MSC complete medium containing 10% dimethyl sulfoxide (DMSO, Sigma-Aldrich). Samples of the passage-2 MCB were submitted for testing including sterility, mycoplasma, and porcine virus testing (9CFR 113). Flow cytometry analysis was performed on passage-2 MCB as previously described [28]. Briefly, single cell suspensions of MSCs were stained with anti-CD14 APC (Miltenyi Biotec), anti-CD29 phycoerythrin (PE), anti-CD105 PE, and anti-CD106 PE (Abcam, Cambridge, MA, USA) and analyzed by Accuri C6 flow cytometer (BD, Carlsbad, CA, USA) using FlowJo software (Tree Star, Ashland, OR, USA). Fc receptors were blocked with Fc Receptor Blocking Agent (Miltenyi Biotech, Auburn, CA, USA), and control staining included isotype-matched monoclonal antibodies (Supplemental Data Figure 1).

The final MSC product was produced by thawing and expanding the passage 2 master cell bank to passage 5 in Cell Factories (Nunc, Thermo Scientific, Waltham, MA). The MSCs were seeded in Cell Factories at a density of 2×10^3 cells/cm^2. MSC complete media was replaced every 2–4 days until reaching 80–90 % confluence and passaged using TrypLE Select (Life Technologies). The final product was cryopreserved at a concentration 1×10^8 per 20 mL Plasma-Lyte A (Baxter, Deerfield, IL) containing 10 % DMSO and 10 % human serum albumin (HSA) (Baxter). The passage 5 MSC product passed sterility testing and was negative for mycoplasma and endotoxin (LAL).

MSC Delivery

Intravenous Infusion (Day 2)—Animals were sedated with intramuscular injection of Telazol 4–6 mg/kg and Xylazine 2 mg/kg, intubated, and mechanically ventilated with 1–3 % isoflurane. An 18G intravenous cannula was placed in an ear vein and flushed. Using aseptic technique, allogeneic MSC (1×10^8) were rapidly thawed in a 37° water bath, diluted with 30 mL of Plasma-Lyte A and 5 % HSA (50 mL total volume) in the bag, and mixed by

gentle inversion. The MSC cell product was attached to standard IV tubing and infused at 2 mL/min. The bag was manually massaged every 10 min to prevent cell settling. ECG, temperature, oxygen saturation, and expired CO_2 were continuously monitored during infusion. Upon completion of MSC infusion, 10 mL of saline was used to flush the IV line over 1 min. To ensure complete anesthetic recovery and apparent health, animals were recovered and observed for 1 h.

Targeted Transendocardial Injection (Day 14)—Using aseptic technique, allogeneic MSC (1×10^8) were rapidly thawed in a 37 °C water bath and diluted with 30 mL of Plasma-Lyte A and 5 % HSA (50 mL total volume). MSCs were transferred from the IV bag with a 60-cm^3 syringe and an 18-gauge needle, placed into a 50-mL conical tube, and centrifuged at $2500 \times g$ for 5 min at 4 ° C. Supernatant was removed, MSCs were suspended in 25 mL Plasma-Lyte A/5 % HAS, and then centrifuged at $2500 \times g$ for 5 min at 4 °C. The supernatant was removed, and the cells suspended in 2.8 mL Plasma-Lyte A and 5% HSA then loaded into three 1 mL Luer Lock syringes using a 20-gauge needle. MSCs were kept at room temperature with intermittent gentle agitation until injection.

Transendocardial MSC injection was performed using the Helix corkscrew-shaped infusion needle and the Morph Universal Deflectable Guide Catheter (BioCardia Inc., San Carlos, CA). MSC and catheter bench-top bio-compatibility was confirmed by injecting 0.2 mL of freshly thawed MSCs over 30 s through 5 different Helix catheters and measuring cell viability by Trypan blue staining and hemocytometer. Pre-injection cell viability immediately following the thawing procedure was 88.9 %. Cell viability was 90.4±0.9 % following delivery through the Helix catheter.

Transendocardial injections were guided by a custom, vendor-independent X-ray fused to MRI (XFM) interventional image co-registration system previously described by our group [26] (Fig. 4a). Briefly, a 3D model of the infarcted and healthy left ventricular endocardium is generated from a pre-op MRI, registered, and overlaid onto a live bi-plane digital X-ray fluoroscopy. The infarct/left ventricle 3D model is also displayed as a 3D volume with inside-the-chamber visualization using interactive cutplanes (Fig. 4b). The shortest distance from the injection catheter tip to infarct distance is automatically available to the operator, and an overview of injection location distribution relative to the infarct is presented as a bulls-eye plot (Fig. 4c). Direct target registration error using this method was determined to be 0.9±5 mm in vivo using injection site co-localization methods [26].

The interventional cardiologist was instructed to inject 0.2 mL of MSC suspension over 30 s with 10 s dwell time for each injection and in a balanced dispersion 0–20 mm from the infarct perimeter. Targeted injection site depth was estimated to be between 33 and 50 % of the wall thickness based on the pre-op MRI, which typically required between 2.5 and 4.5 rotations of the Helix device. Thirty minutes following transendocardial injections, transthoracic echocardiography was performed using a clinical Philips iE33 echo to assess for the development of pericardial effusion.

Ventricular Arrhythmia Surveillance

Continuous multi-lead telemetry monitoring was performed during MI model creation, MSC administration (both intravenous infusion and transendocardial injection), and during MRI imaging. Furthermore, a Reveal XT (Medtronic, Minneapolis, MN) implantable loop recorder was surgically implanted in a small subcutaneous pocket created adjacent to the left scapula. Pilot tests were performed to confirm that the device implanted in this location would not distort cardiac MRI and that MRI radiofrequency would not interfere with ECG recordings. The implanted loop recorder was programmed to detect tachycardia (>176 bpm) for 24 beats, which is the upper detection limit of the device. Scheduled wireless device interrogation was performed on day 2, 14, 21, and 55 following MI. Rhythm strips from every recorded event and at every time point was independently adjudicated and verified by experienced blinded investigators to distinguish ECG artifact from shivering or excess motion, from wide complex tachycardia. It is assumed in the context of an MI model that all abrupt wide complex tachycardia would indicate ventricular tachycardia and not supraventricular tachycardia with aberrant conduction.

Invasive Hemodynamic Endpoints

Invasive pressure-volume loop measurements were performed using a 7F high fidelity multi-ring electrode conductance catheter (Scisense Inc, London, ON) positioned retrograde into the left ventricle via transcarotid artery access. A 24-mm diameter balloon catheter was positioned via femoral vein into the inferior vena cava. Contralateral femoral venous access was obtained to advance a 7F Swan Ganz catheter under fluoroscopic guidance into the pulmonary artery. Calibrating stroke volume estimates were obtained by Swan Ganz thermal dilution method. Pressure–dimension data was recorded at steady state and during transient inferior vena cava occlusion, both at pre-dobutamine and with 20 mcg/kg IV dobutamine infusion. Contractility reserve was defined as the difference in end-systolic pressure-volume relationship (ESPVR) between dobutamine stress and rest.

Myocardial contractility and work was indexed by the maximal rate of isovolumetric contraction (+dP/dt), stroke work (SW), and ventricular elastance, slope of the end-systolic pressure–dimension relationship (Ees). Pre-load was analyzed as end-diastolic dimension and pressure and afterload evaluated as effective arterial elastance (the ratio of LV end-systolic pressure to stroke dimension). Diastolic function was indexed by LV end-diastolic pressure and the time constant of ventricular relaxation (Glantz formula). Hemodynamic pressure–dimension data was digitized at 200 Hz and stored for subsequent analysis on a personal computer by using commercial software (Scisense Inc, London, ON).

Cardiac MRI

Cardiac magnetic resonance maging (MRI) was performed on post-MI day 2, 14, and 55 on a 1.5 T Signa HDx, wide bore MRI (GE Healthcare, Waukesha, WI) using previously described methods [26]. Specifically, left ventricular chamber size and function was measured using short axis oblique slices with balanced steady-state free procession (bSSFP) imaging. (Scan parameters: TR/TE/Flip angle=3.3 ms/1.1 ms/45; field-of-view (FOV)/matrix=35×26 cm/256×144; no. of slices/slice thickness/spacing=20/5 mm/0 mm; cardiac phases/views per segment=20/16). Infarct size was measured using standard delayed

enhancement (DE) inversion recovery based sequence performed 10 min following intravenous administration of 0.15 mmol/kg Gd-BOPTA (Multihance, Bracco Diagnostics, Princeton, NJ). (Scan parameters: TR/TE/TI/Flip angle=6.5 ms/1.7 ms/200–280 ms/20°; FOV/Matrix=35× 26 cm/256×144; number of slices/slice thickness/spacing= 20/5 mm/0 mm; views per heartbeat=32). The trigger delay was adjusted to image mid-diastole based on the multiphase bSSFP series. All MRI imaging was performed at end expiration by temporarily suspending mechanical ventilation.

Anatomic and functional cardiac image analysis was performed using QMass 7.5 software (Medis, Leiden, The Netherlands) by two experienced investigators who were blinded to treatment assignment.

Blood Counts and Serology

Blood was drawn from swine at days 0, 2, 14, 21, and 55 via jugular vein and collected in EDTA and serum-separating tubes for complete blood count and serology. Serology samples were allowed to clot on ice for 1 h. Samples were centrifuged at 1000×g for 10 min, serum aspirated, and frozen at −80 until analysis. Serum was analyzed for TNF alpha (R&D Systems, PTA00), IL-6 (R&D Systems, P6000B), IL-10 (R&D Systems, P1000), and IL-12 (AbCam, ab156506) according to the manufacturers' protocols.

Histopathology

On day 55 post-MI, hearts were excised, rinsed in saline, and sectioned on the short access from apex to base in 1 cm increments. Heart slices were digitally imaged then placed in 10 % neutral buffered formalin for 24 h before transfer to 70 % ethanol until trimming and histological processing. Histological analysis was carried out on the second slice proximal to the apex, where the infarct was the most noticeable. This slice was trimmed to create six sections; one cross-section of the left ventricular infarct with adjacent affected interventricular septum and right ventricle, four longitudinal sections progressing radially from the grossly apparent left ventricular infarct along the left ventricular free wall (approximately 1 cm^2 each and 5–8 mm apart), and a section of unaffected interventricular septum (approximately 1 cm^2).

Each section was stained with H&E and Masson's Trichrome and quantitatively graded for infarction, myocardial hemorrhage, foci of hemosiderophages, lymphocytic foci, granulomatous or histiocytic foci, fatty infiltration/degeneration, ventricular myofiber anisokaryosis, left ventricular subepicardial fibrosis, left ventricular myocardial fibrosis, left ventricular subendocardial fibrosis, myocardial mineralization, and epicardial fibrovascular tissue by a blinded board-certified veterinary pathologist (D.S.). (Supplemental Methods Table 1). Capillary density was assessed by counting single red blood cells as proxies for capillaries in five 400× fields bordering the fibrotic areas on H&E-stained slides by a blinded board-certified veterinary pathologist (D.S.) as described by previous reports [29, 30].

Myocardial infarct border segments from each female pig were analyzed for male donor pig MSCs by fluorescent in situ hybridization (FISH) for the presence of Y chromosome using a porcine X and Y probe (Zytovision, Z-2094-200) and a commercial kit (Kreatech,

KI-60007) by blinded investigators. Signals for 100 cells were counted from 5 distinct high-powered fields following the x-axis of each slide encompassing the length of the tissue section.

Statistical Methods

Mixed effects models with repeated measures were used to examine the treatment and time effects on repeated MRI measurements and blood measurements, respectively. Least square means with standard errors for the four treatments at each time point were calculated, and pairwise comparisons among four treatments are conducted by t tests. General linear models were used to examine the treatment effects on pressure-volume measurements at rest and pressure-volume measurements at stress. Similarly, least square means and standard errors for the four treatments were calculated, and pairwise comparisons among four treatments were conducted by t tests. The effects of the four treatments on contractility were examined by analysis of covariance adjusting for (day 2 post-MI) ejection fraction, end-systolic volume, and the percent LV infarcted. The effects of IV MSC treatment compared with IV placebo on median time to first arrhythmia were examined from day 2 to day 14 and from day 14 to day 55 by log-rank test. The effects of all four treatments on the time to first arrhythmia from day 14 to day 55 were examined by log-rank test.

Results

Thirty-six swine had antero-septal MI induced; however, 12 died within the first 12 h following coronary artery occlusion due to ventricular fibrillation despite aggressive resuscitation efforts. The 12 animals that died were neither randomized nor treated with study agents and were excluded from all data analysis. One pig assigned to the IV placebo plus TE MSC (−+) group died at 27 days post-MI of ventricular tachycardia that degenerated to ventricular fibrillation. In this animal, the implanted loop recorder revealed frequent sustained ventricular tachycardia episodes immediately following MI model creation but before treatment. Therefore, all 24 swine completed the treatment phase; however, 55-day follow-up was complete on 23 swine.

Intravenous and transendocardial delivery of MSCs was successfully performed without significant alterations in heart rate, body temperature, oxygen saturation, and end tidal CO_2 in all animals. Twelve to fourteen XFM-guided transendocardial injections were performed per animal. The mean procedure time from the start of femoral introducer sheath insertion to the end of the final injection was 27.9± 1.5 min, and total fluoroscopy time was 13.8±0.5 min. Post-TE injection transthoracic echocardiography showed no pericardial effusion in any animals.

Invasive Hemodynamics and Pressure-Volume Relationships

Pre-load independent contractile reserve (defined as the difference between stress and rest end-systolic pressure-volume relationship or ESPVR) following intravenous dobutamine challenge was significantly improved for the IV MSC plus TE MSC (++) group compared to all other groups (p=0.02) (Fig. 2). Although rest ESPVR was the greatest in the IV MSC plus TE placebo (+−) group (p=0.001), this group also suffered the lowest contractile reserve

with dobutamine challenge (p=0.02). There was no statistically significant interaction between contractile reserve and percent infarct (p=0.57), end-systolic volume (p=0.99), or ejection fraction (p=0.17) measured by MRI at day 2 post-MI (Supplemental Data Table 1).

MRI Endpoints

Day 2 post-MI ejection fraction was lower in the IV placebo plus TE placebo group (−−) (27.7±2.8 %) compared to IV placebo plus TE MSC (−+) (39.0±3.1 %) (p=0.01), IV MSC plus TE placebo group (+−) (42.0±2.8 %) (p=0.001), and IV MSC plus TE MSC group (40.2±2.8 %) (p=0.003) despite blinded treatment randomization. In addition, infarct volume was greater in the IV placebo plus TE placebo group (−−) (21.3±2.0 mL) compared with IV MSC plus TE MSC group (++) (16.5±1.3 mL) (p=0.02), but was statistically similar to the other groups. There were no detectable inter-group differences in the change in infarct size when measured as an absolute volume and as a percent of left ventricular myocardial volume (Fig. 3). Furthermore, there were no inter-group differences for change in end-systolic volume, end-diastolic volume, stroke volume, and global ejection fraction for day 55–2, day 55–14, and day 14–2 comparisons (Supplemental Data Table 2).

Transendocardial Injection Targeting Success

The XFM co-registration system was successfully used to guide all 24 transendocardial injection procedures (Fig. 4a–d). Ninety-three percent of all transendocardial injections were administered within the pre-specified 0–20 mm infarct perimeter, with no significant inter-group differences (p=0.29). No injections were localized within the infarct itself, and 7.3 % of all injections were localized outside of the 20 mm infarct perimeter. There were no significant differences in distribution pattern (diffuse vs. clustered) of injections around the infarct zone between all 4 groups. The mean injection depth from the endocardium was 3.2±0.2 mm, epicardium 5.5±0.4 mm, and the mean distance to infarct was 8.9±0.5 mm. There were no significant differences in mean injection depth or distance to infarct in any treatment group (Fig. 4e).

Ventricular Arrhythmias

Sustained fast VT (defined as >30 s of wide complex tachycardia at greater than 176 bpm) episodes were common in this porcine MI model. Overall, the greatest sustained fast VT burden occurred in the first several days post-MI and declined in the weeks that followed. The IV MSC plus TE MSC (++) group was superior to all other groups for freedom of sustained fast VT at day 55 compared to day 2 post-MI (Fig. 5).

The sustained fast VT burden was further analyzed based on the time periods from day 2 to day 14 post-MI (to evaluate the early impact of IV MSC therapy) (Fig. 5a) and from day 14 to day 55 post-MI (to evaluate the late impact of combination IV and TE MSC therapy) (Fig. 5b). In the early time period (day 2 to day 14), there was no difference in time to first sustained fast VT between IV placebo treated swine (n=12) and IV MSC treated swine (n=12), (12 vs 7.5 days respectively, p=0.57). In the time period between day 14 and day 55, the time to the first sustained fast VT was significantly improved for the IV MSC and TE MSC (++) group (p=0.03) compared to other groups. Specifically, the IV placebo plus TE placebo (−−) group had a median time to the first sustained fast VT of 1 day, IV MSC plus

TE placebo (+−) has a median time to the first arrhythmia of 0 day, IV placebo plus TE MSC (−+) group had a median time to the first sustained fast VT of 20.5 days, and IV MSC plus TE MSC (++) group had a median time to the first sustained fast VT of >41 days.

Laboratory and Histopathology Results

Inflammatory Markers—Serial analysis of total nucleated cells, neutrophils, lymphocytes, and the inflammatory markers TNFalpha, IL-6, IL-10, and IL-12 was carried out on days 0, 2, 14, 21, and 55. There were no significant changes over time within each pig or between treatment groups in any markers analyzed (Supplemental Data Figure 2).

Gross Necropsy Findings—There were no inter-group differences in body weight (p=0.43), heart weight (p=0.18), and heart-weight to body-weight ratio (p=0.29). There was no evidence of pericardial effusion, gross lung, liver, spleen pathology, or ectopic tumor formation at day 55 (Supplemental Data Table 3).

Light Microscopy—The group that received IV MSC plus TE MSC (++) had a significantly increased number of lymphocytic foci compared to all other groups (p=0.002) (Fig. 6a – d), and this difference was the greatest in the peri-infarct zone. Epicardial fibrovascular tissue was reduced in all three MSC treatment groups compared to the total placebo control (p=0.009) with no intergroup differences in the MSC groups. There was no difference in capillary density in the peri-infarct tissue adjacent to the fibrotic tissue (border zone) IV placebo plus TE placebo (−−) (74.6±5.7), IV MSC plus TE placebo (+−) (70.63±5.3), IV placebo plus TE MSC (−+) (65.6±4.8), and IV MSC plus TE MSC (++) (69.7±7.0). Finally, there were no significant differences identified in myocardial hemorrhage, hemosiderophage foci, granulomatous or histocytic foci, fatty infiltration/ degeneration, myofiber anisokaryosis, left ventricular subepicardial fibrosis, left ventricular myocardial fibrosis, left ventricular subendocardial fibrosis, or myocardial mineralization (Supplemental Data Figure 3).

Fluorescent In Situ Hybridization—By day 55, there was no identifiable sex-mismatched donor MSCs in any animal of the 3 groups receiving MSCs.

Discussion

To our knowledge, this is the first large animal translational study to examine *repeated* dosing of allogeneic MSCs post-MI. In addition, this was the first therapeutic *efficacy* study that utilized a multi-modality image co-registration system for efficient and accurate transendocardial injections into the discrete infarct border zone. Furthermore, cardiac *contractility* reserve has not been explored in prior post-MI pre-clinical and clinical trials. Finally, rigorous monitoring for VT by an implantable ECG recorder in a translational therapeutic study was successfully accomplished for the first time and is a significant step forward for VT monitoring in clinically translatable large animal models.

This large animal study was designed to test the *biologically plausible* and *clinically practical* hypothesis that a therapeutic delivery strategy of early IV MSC infusion, later followed by *targeted* TE MSC injection could improve contractility reserve and prevent

adverse remodeling post-MI. We observed that this novel MSC deliver approach resulted in significantly improved contractility reserve. This improvement cannot be explained as a dose-related effect since contractility reserve in the IV placebo plus TE MSC (−+) group was not different compared to the control (−−) group. Furthermore, the IV MSC plus TE placebo group (+−) had *worse* contractility reserve compared to the control (−−) group. Additionally, we observed that sustained fast VT was dramatically reduced with serial MSC treatment in this MI model.

Contrary to other reports [21, 31–33], we observed that allogeneic MSC administration had no measurable effect on infarct volume, left ventricular chamber volumes, or ejection fraction. Differences in the strain of swine used, cell type and dose, timing of cell administration, route of administration, and the novel use of MRI to X-ray co-registration imaging to target TE delivery may explain these discrepancies. On the other hand, our findings are consistent with the clinical experience to date [17, 19, 20, 34–38] where safety of MSC administration and suppression of ventricular arrhythmias has been observed without large improvements in LV dimension or ejection fraction.

Potential Mechanisms Underlying Improvements in Contractile Reserve

Myocardial contractility reserve predicts improved survival in humans with ischemic cardiomyopathy and is a better predictor of future adverse clinical outcomes compared to infarct size in patients with large MI [39, 40]. Factors that lead to poor post-MI contractility reserve and subsequently poor clinical outcome include dysregulation of beta adrenergic receptor signaling through increased G-protein coupled receptor kinase expression [41–44] and disordered calcium channel function [45]. MSC therapy may heighten sensitivity to catecholamine stimulation through increased beta adrenergic receptor expression, increased receptor sensitivity, or enhanced myocyte recruitment. Factors shown to restore contractility reserve following MI include VEGF-induced angiogenesis and reduced cardiac GRK2 levels associated with exercise [46]. In addition, a link between neo-angiogenesis and enhanced beta-2 adrenergic receptor expression in ischemic skeletal muscle was previously suggested by Iaccarino et al. [47]. However, in the present study, no differences were observed in vessel density suggesting there may be alternative mechanisms to explain cardiac myocyte recruitment with serial MSC therapy.

Serial Allogeneic MSC Therapy Induces a Local Lymphoproliferative Response

Excess accumulation of lymphocytic foci in the infarct and border regions was observed in the double MSC treated group (++) compared to all other groups (Fig. 6c). This occurred despite no evidence of a systemic inflammatory response by serum levels of inflammatory proteins, blood lymphocyte levels, or histologic presence of identifiable intact MSCs. A potential explanation is that a persistent, low-grade allogeneic immune response persists with serial double dose MSC treatment. There was no safety issues observed with this observation and in fact, serial MSC treatment *suppressed* ventricular arrhythmias. While it has been suggested that MSCs suppress premature ventricular contractions in animal and humans, [21, 48] the mechanism of how this occurs remains unknown.

Limitations

Myocardial perfusion is a key component to preventing post-MI remodeling. In this study, a coronary occlusion reperfusion model was chosen to mimic clinical practice where stent revascularization is performed. Our results do not extend to the situation where the culprit coronary artery remains occluded. Further, juvenile swine rather than older miniature swine were used due to cost. Longer follow-up was not possible as these swine become too large for MRI. Although the sample size is small compared to human efficacy trials, it is comparable to other published large animal translational studies [27, 33, 49, 50]. Our study exploited highly sensitive and reproducible endpoints such as quantitative cardiac MRI, invasive pressure-volume hemodynamics, implanted VT monitoring, and systematic histopathology to compensate for the small sample size. In addition, beta-blocker and angiotensin converting enzyme inhibitor therapy was not administered during the follow-up period as would be standard if this were a human trial. Therefore, the findings in this study cannot be extrapolated if these anti-remodeling therapies were administered. Despite random assignment, day 2 post-MI differences in ejection fraction and infarct volume were observed. Although not commonly performed in large animal studies, excluding animals from treatment assignment on the basis of thresholds in baseline (day 2 post-MI) measurements would ensure balance between groups. Mechanisms underlying the observation of improved contractility reserve, reduced VT burden, and lymphocytic foci in the peri-infarct zone in the serial MSC therapy group were not explored in detail due to funding constraints. Further studies that put these effects into mechanistic context are required.

Conclusions

In a swine MI model, early intravenous infusion later followed by targeted transendocardial injection of allogeneic bone marrow-derived mesenchymal stem cells improves contractility reserve and suppresses sustained ventricular tachycardia but does not affect infarct size, LV end-systolic volume, LV end-diastolic volume, or ejection fraction. Multi-modality X-ray fused with MRI interventional co-registration successfully and efficiently enabled targeted transendocardial cell therapy precisely into the infarct border. Human trials are warranted to confirm these results.

Supplementary Material

Refer to Web version on PubMed Central for supplementary material.

Acknowledgments

Abbreviations

MI	Myocardial infarction
MSC	Mesenchymal stem cell
XFM	X-ray fused to MRI
IV	Intravenous
TE	Transendocardial
LAD	Left anterior descending
MRI	Magnetic resonance imaging

References

1. Burchfield JS, Xie M, Hill JA. Pathological ventricular remodeling: mechanisms: part 1 of 2. Circulation. 2013; 128(4):388–400. [PubMed: 23877061]

2. Xie M, Burchfield JS, Hill JA. Pathological ventricular remodeling: therapies: part 2 of 2. Circulation. 2013; 128(9):1021–1030. [PubMed: 23979628]

3. Yeh RW, et al. Population trends in the incidence and outcomes of acute myocardial infarction. New England Journal of Medicine. 2010; 362(23):2155–2165. [PubMed: 20558366]

4. Goodrich AD, Hematti P. Mesenchymal stem cell therapies: the quest for fine-tuning. Experimental Dermatology. 2014; 23(9):632–633. [PubMed: 24806552]

5. Pittenger MF, et al. Multilineage potential of adult human mesenchymal stem cells. Science. 1999; 284(5411):143–147. [PubMed: 10102814]

6. Aggarwal S, Pittenger MF. Human mesenchymal stem cells modulate allogeneic immune cell responses. Blood. 2005; 105(4):1815–1822. [PubMed: 15494428]

7. Cho DI, et al. Mesenchymal stem cells reciprocally regulate the M1/M2 balance in mouse bone marrow-derived macrophages. Experimental & Molecular Medicine. 2014; 46:e70. [PubMed: 24406319]

8. Kim J, Hematti P. Mesenchymal stem cell-educated macrophages: a novel type of alternatively activated macrophages. Experimental Hematology. 2009; 37(12):1445–1453. [PubMed: 19772890]

9. Hanson SE, Kim J, Hematti P. Comparative analysis of adipose-derived mesenchymal stem cells isolated from abdominal and breast tissue. Aesthetic Surgery Journal. 2013; 33(6):888–898. [PubMed: 23908304]

10. Lushaj EB, et al. Mesenchymal stromal cells are present in the heart and promote growth of adult stem cells in vitro. Cytotherapy. 2011; 13(4):400–406. [PubMed: 21090918]

11. Le Blanc K, et al. HLA expression and immunologic properties of differentiated and undifferentiated mesenchymal stem cells. Experimental Hematology. 2003; 31(10):890–896. [PubMed: 14550804]

12. Ryan JM, et al. Mesenchymal stem cells avoid allogeneic rejection. Journal of Inflammation (London). 2005; 2:8.

13. Zimmet JM, Hare JM. Emerging role for bone marrow derived mesenchymal stem cells in myocardial regenerative therapy. Basic Research in Cardiology. 2005; 100(6):471–481. [PubMed: 16237508]

14. Atoui R, et al. Marrow stromal cells as universal donor cells for myocardial regenerative therapy: their unique immune tolerance. Annals of Thoracic Surgery. 2008; 85(2):571–579. [PubMed: 18222266]

15. Poh KK, et al. Repeated direct endomyocardial transplantation of allogeneic mesenchymal stem cells: safety of a high dose, "off-the-shelf", cellular cardiomyoplasty strategy. International Journal of Cardiology. 2007; 117(3):360–364. [PubMed: 16889857]

16. Uccelli A, Moretta L, Pistoia V. Mesenchymal stem cells in health and disease. Nature Reviews Immunology. 2008; 8(9):726–736.

17. Beitnes JO, et al. Long-term results after intracoronary injection of autologous mononuclear bone marrow cells in acute myocardial infarction: the ASTAMI randomised, controlled study. Heart. 2009; 95(24):1983–1989. [PubMed: 19833610]

18. Leistner DM, et al. Transplantation of progenitor cells and regeneration enhancement in acute myocardial infarction (TOPCARE-AMI): final 5-year results suggest long-term safety and efficacy. Clinical Research in Cardiology. 2011; 100(10):925–934. [PubMed: 21633921]

19. Traverse JH, et al. Effect of intracoronary delivery of autologous bone marrow mononuclear cells 2 to 3 weeks following acute myocardial infarction on left ventricular function: the LateTIME randomized trial. JAMA. 2011; 306(19):2110–2119. [PubMed: 22084195]

20. Meyer GP, et al. Intracoronary bone marrow cell transfer after myocardial infarction: 5-year follow-up from the randomized-controlled BOOST trial. European Heart Journal. 2009; 30(24): 2978–2984. [PubMed: 19773226]

21. Hare JM, et al. A randomized, double-blind, placebo-controlled, dose-escalation study of intravenous adult human mesenchymal stem cells (prochymal) after acute myocardial infarction. Journal of the American College of Cardiology. 2009; 54(24):2277–2286. [PubMed: 19958962]

22. Vandervelde S, et al. Signaling factors in stem cell-mediated repair of infarcted myocardium. Journal of Molecular and Cellular Cardiology. 2005; 39(2):363–376. [PubMed: 15992820]

23. Abbott JD, et al. Stromal cell-derived factor-1alpha plays a critical role in stem cell recruitment to the heart after myocardial infarction but is not sufficient to induce homing in the absence of injury. Circulation. 2004; 110(21):3300–3305. [PubMed: 15533866]

24. Ma J, et al. Time course of myocardial stromal cell-derived factor 1 expression and beneficial effects of intravenously administered bone marrow stem cells in rats with experimental myocardial infarction. Basic Research in Cardiology. 2005; 100(3):217–223. [PubMed: 15754085]

25. Lee RH, et al. Intravenous hMSCs improve myocardial infarction in mice because cells embolized in lung are activated to secrete the anti-inflammatory protein TSG-6. Cell Stem Cell. 2009; 5(1): 54–63. [PubMed: 19570514]

26. Tomkowiak MT, et al. Targeted transendocardial therapeutic delivery guided by mri-x-ray image fusion. Catheterization and Cardiovascular Interventions. 2011; 78(3):468–478. [PubMed: 21413125]

27. de Silva R, et al. Intracoronary infusion of autologous mononuclear cells from bone marrow or granulocyte colony-stimulating factor-mobilized apheresis product may not improve remodelling, contractile function, perfusion, or infarct size in a swine model of large myocardial infarction. European Heart Journal. 2008; 29(14):1772–1782. [PubMed: 18502738]

28. Hanson SE, et al. Local delivery of allogeneic bone marrow and adipose tissue-derived mesenchymal stromal cells for cutaneous wound healing in a porcine model. Journal of Tissue Engineering and Regenerative Medicine. 2013

29. Tomita S, et al. Autologous transplantation of bone marrow cells improves damaged heart function. Circulation. 1999; 100(19 Suppl):II247–II256. [PubMed: 10567312]

30. Tang J, et al. Mesenchymal stem cells participate in angiogenesis and improve heart function in rat model of myocardial ischemia with reperfusion. European Journal of Cardio-Thoracic Surgery. 2006; 30(2):353–361. [PubMed: 16829080]

31. Amado LC, et al. Cardiac repair with intramyocardial injection of allogeneic mesenchymal stem cells after myocardial infarction. Proceedings of the National Academy of Sciences of the United States of America. 2005; 102(32):11474–11479. [PubMed: 16061805]

32. Hare JM, et al. Comparison of allogeneic vs autologous bone marrow-derived mesenchymal stem cells delivered by transendocardial injection in patients with ischemic cardiomyopathy: the POSEIDON randomized trial. JAMA. 2012; 308(22):2369–2379. [PubMed: 23117550]

33. Williams AR, et al. Durable scar size reduction due to allogeneic mesenchymal stem cell therapy regulates whole-chamber remodeling. Journal of American Heart Association. 2013; 2(3):e000140.

34. Kuethe F, et al. Lack of regeneration of myocardium by autologous intracoronary mononuclear bone marrow cell transplantation in humans with large anterior myocardial infarctions. International Journal of Cardiology. 2004; 97(1):123–127. [PubMed: 15336818]

35. Heldman AW, et al. Transendocardial mesenchymal stem cells and mononuclear bone marrow cells for ischemic cardiomyopathy: the TAC-HFT randomized trial. JAMA. 2014; 311(1):62–73. [PubMed: 24247587]

36. Arnold R, et al. Absence of accelerated atherosclerotic disease progression after intracoronary infusion of bone marrow derived mononuclear cells in patients with acute myocardial infarction—angiographic and intravascular ultrasound—results from the TErapia Celular Aplicada al Miocardio Pilot study. American Heart Journal. 2010; 159(6):1154, e1–e8. [PubMed: 20569733]

37. Surder D, et al. Cell-based therapy for myocardial repair in patients with acute myocardial infarction: rationale and study design of the SWiss multicenter Intracoronary Stem cells Study in Acute Myocardial Infarction (SWISS-AMI). American Heart Journal. 2010; 160(1):58–64. [PubMed: 20598973]

38. Perin EC, et al. Effect of transendocardial delivery of autologous bone marrow mononuclear cells on functional capacity, left ventricular function, and perfusion in chronic heart failure: the FOCUS-CCTRN trial. JAMA. 2012; 307(16):1717–1726. [PubMed: 22447880]

39. Chaudhry FA, et al. Prognostic implications of myocardial contractile reserve in patients with coronary artery disease and left ventricular dysfunction. Journal of the American College of Cardiology. 1999; 34(3):730–738. [PubMed: 10483954]

40. Kelle S, et al. Prognostic value of myocardial infarct size and contractile reserve using magnetic resonance imaging. Journal of the American College of Cardiology. 2009; 54(19):1770–1777. [PubMed: 19874990]

41. Petrofski JA, Koch WJ. The beta-adrenergic receptor kinase in heart failure. Journal of Molecular and Cellular Cardiology. 2003; 35(10):1167–1174. [PubMed: 14519424]

42. Ungerer M, et al. Altered expression of beta-adrenergic receptor kinase and beta 1-adrenergic receptors in the failing human heart. Circulation. 1993; 87(2):454–463. [PubMed: 8381058]

43. Woodall MC, et al. G protein-coupled receptor kinase 2: a link between myocardial contractile function and cardiac metabolism. Circulation Research. 2014; 114(10):1661–1670. [PubMed: 24812353]

44. Bristow MR, et al. Decreased catecholamine sensitivity and beta-adrenergic-receptor density in failing human hearts. The New England Journal of Medicine. 1982; 307(4):205–211. [PubMed: 6283349]

45. Makarewich CA, et al. Transient receptor potential channels contribute to pathological structural and functional remodeling after myocardial infarction. Circulation Research. 2014; 115(6):567–580. [PubMed: 25047165]

46. Leosco D, et al. Exercise promotes angiogenesis and improves beta-adrenergic receptor signalling in the post-ischaemic failing rat heart. Cardiovascular Research. 2008; 78(2):385–394. [PubMed: 18093988]

47. Iaccarino G, et al. Ischemic neoangiogenesis enhanced by beta2-adrenergic receptor overexpression: a novel role for the endothelial adrenergic system. Circulation Research. 2005; 97(11):1182–1189. [PubMed: 16239589]

48. Wang D, et al. Intracoronary delivery of mesenchymal stem cells reduces proarrhythmogenic risks in swine with myocardial infarction. Irish Journal of Medical Science. 2011; 180(2):379–385. [PubMed: 21286844]

49. Schuleri KH, et al. Autologous mesenchymal stem cells produce reverse remodelling in chronic ischaemic cardiomyopathy. European Heart Journal. 2009; 30(22):2722–2732. [PubMed: 19586959]

50. Williams AR, et al. Enhanced effect of combining human cardiac stem cells and bone marrow mesenchymal stem cells to reduce infarct size and to restore cardiac function after myocardial infarction. Circulation. 2013; 127(2):213–223. [PubMed: 23224061]

Clinical Relevance Statement

There is evidence to suggest that single dose administration of bone marrow-derived mesenchymal stem cells for the treatment of myocardial infarction offers short-term benefit. In clinical practice, serial dosing may be required; however, this has not been tested in pre-clinical models. Our data suggest that a biologically plausible and clinically practical delivery approach of intravenous followed by transendocardial catheter delivery of bone marrow-derived mesenchymal stem cells improves contractile reserve and suppresses ventricular arrhythmias.
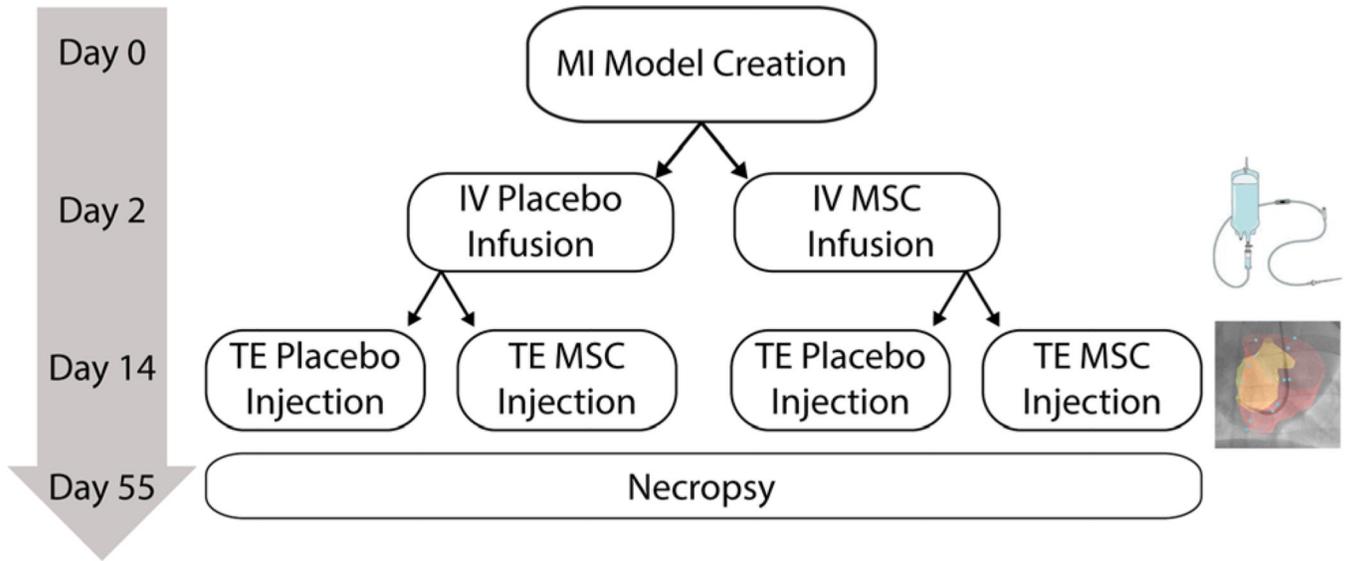
Fig. 1.
Myocardial infarction was induced by closed chest, balloon occlusion reperfusion of the LAD. Thirty-six Yorkshire swine underwent 90 min of ischemia. Twenty-four animals survived the model creation to be randomized into treatment groups. Two days post-MI swine underwent a cardiac MRI and were given either an IV infusion of porcine MSCs or a placebo. Fourteen days post-MI swine underwent a second cardiac MRI and received XFM guided transendocardial (TE) MSC injections or placebo injections. The study design resulted in four treatment groups: IV placebo plus TE placebo (−−) (n=6), IV placebo plus TE MSC (−+) (n=6), IV MSC plus TE placebo (+−) (n=6), and IV MSC plus TE MSC (++) n=6). Swine were survived out to 55 days post-MI at which time a follow-up cardiac MRI and invasive pressure-volume loop analysis was carried out prior to necropsy
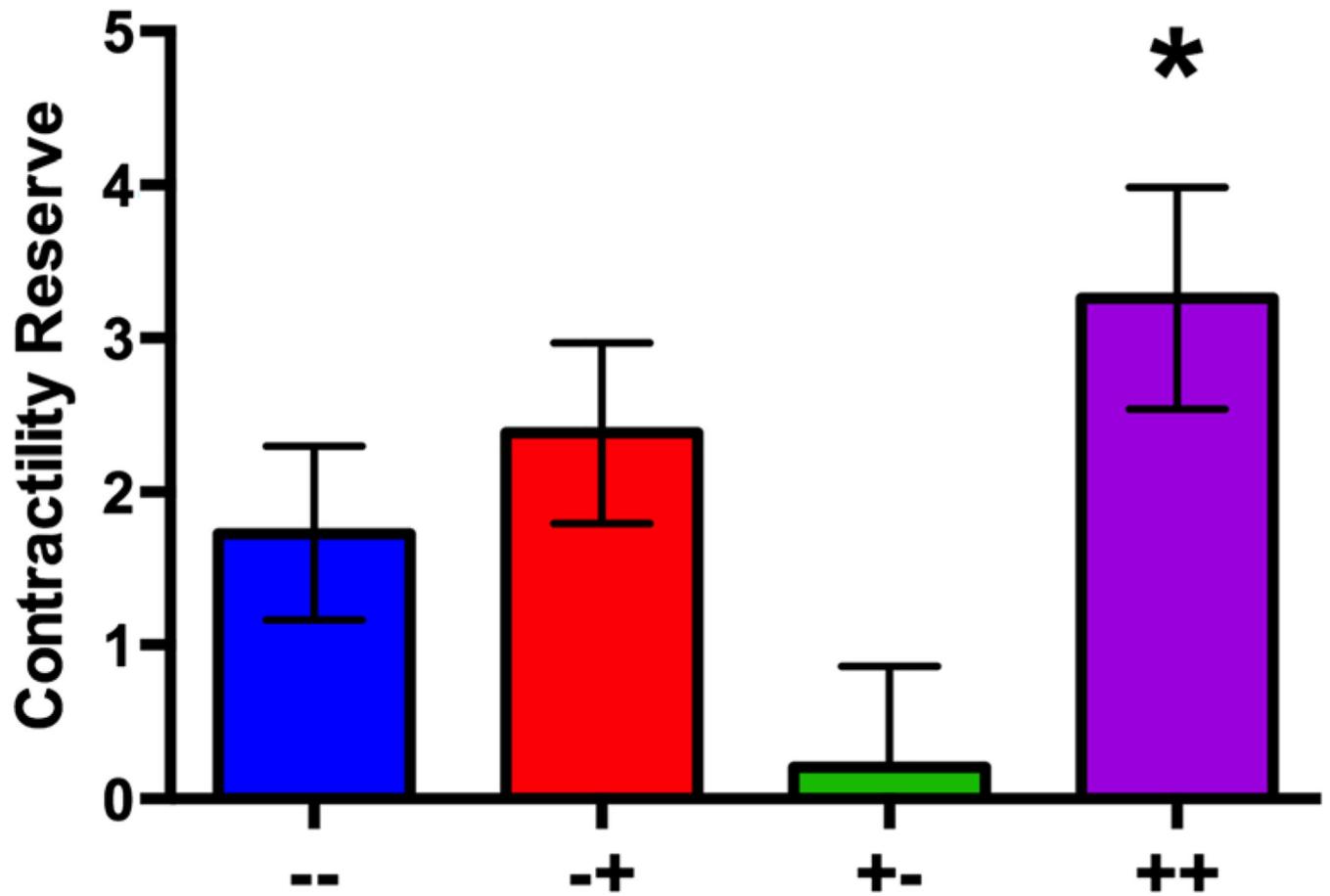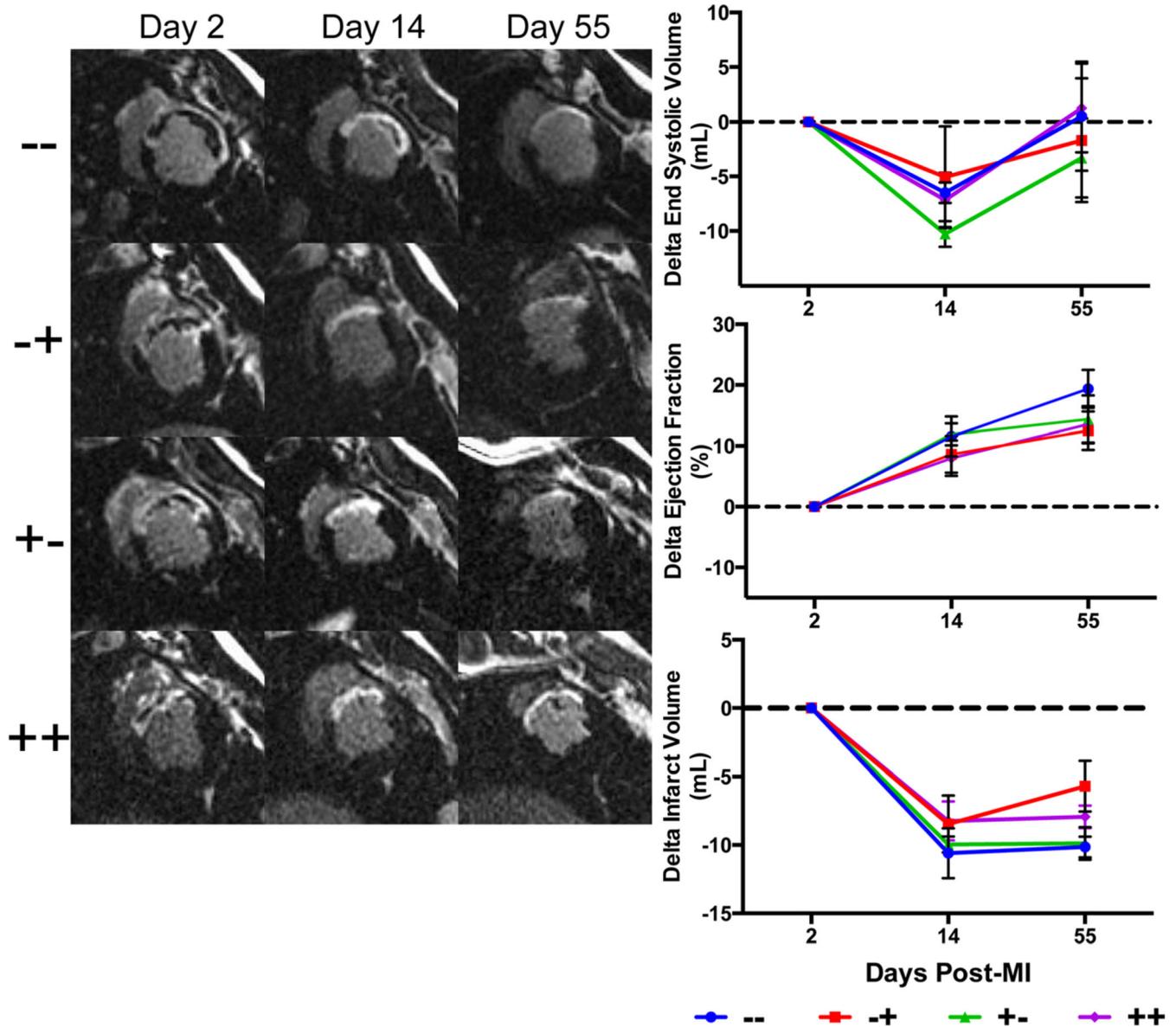
Fig. 2.
a Contractile reserve measured was the greatest in the IV MSC plus TE MSC group (++ compared to all others (*p=0.02) and the worst in the IV MSC plus TE placebo group (+−)

Fig. 3.
Representative delayed enhancement cardiac MRI images at 2, 14 and 55 days post-MI for each group. Note the thinning of the infarct (white section of the LV wall) and dilation of the LV between day 2 and 55. End-systolic volumes (*top*) were reduced at day 14, but returned to baseline (day 2 post-MI) by day 55. Ejection fractions (*middle*) increased in all groups at day 14 and 55 compared to day 2 post-MI due to myocardial stunning effects. Infarct volumes reduced from day 2 to day 14 due to resolving myocardial edema. IV placebo plus TE placebo (−−), IV Placebo plus TE MSC (−+), IV MSC plus TE placebo (+−), IV MSC plus TE MSC (++)
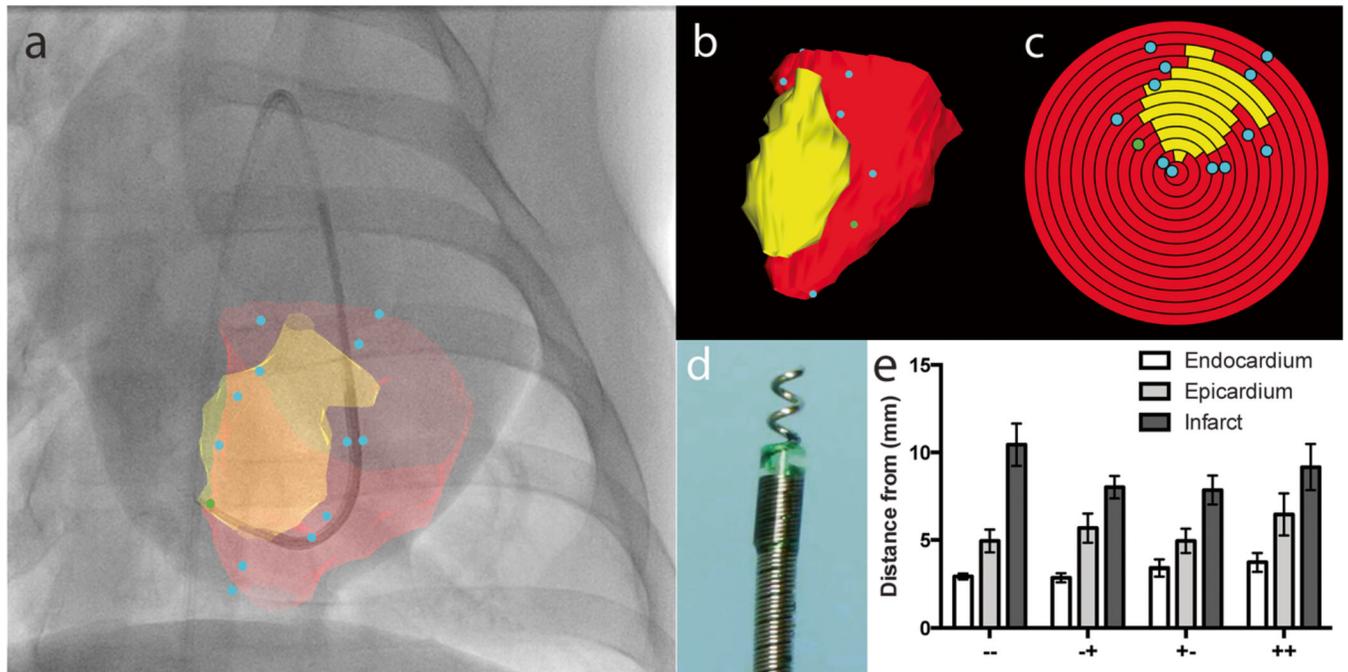
Fig. 4.
Bi-plane X-ray fluoroscopy fused with MRI guided transendocardial injections. **a**
Intraoperative display of MRI endocardial (*red*) and infarct (*yellow*) surface registered and
projected on to live X-ray fluoroscopy in the anterior-posterior view. *Blue dots* indicate the
injection locations. **b** Three dimensional surface rendered volume in an oblique view and **c**
corresponding polar plot of injection locations. The apex of the ventricle represents the
center of the polar plot. **d** Corkscrew-shaped needle tipped Helix transendocardial injection
catheter. **e** Mean distances of injection location to the closest endocardial, epicardial, and
infarct surface across all treatment groups. IV placebo plus TE placebo (−−), IV Placebo
plus TE MSC (−+), IV MSC plus TE placebo (+−), and IV MSC plus TE MSC (++)
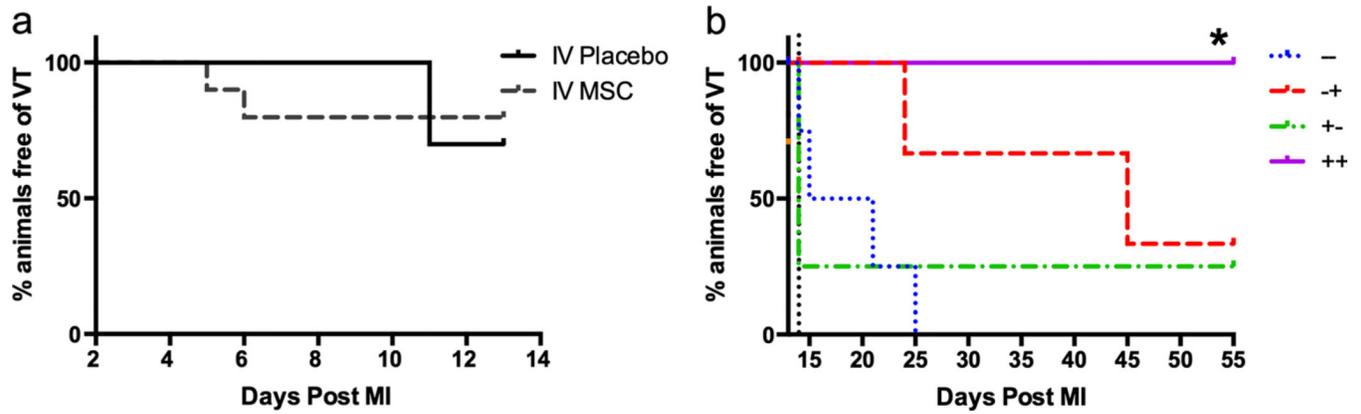
Fig. 5.
Time to sustained fast ventricular tachycardia. **a** Day 2 to day 14 analysis on the effects of
IV MSC therapy on median time to first ventricular tachycardia event (IV placebo (n=12)
and IV MSC (n=12)). IV MSC treatment had no significant effect on median time to
sustained fast ventricular tachycardia (p=0.56). **b** Day 14 to day 55 analysis: When data was
analyzed from day 14 (The *vertical dotted black line*), there was a significant reduction in
VT in the ++ group compared to other groups (p=0.033)
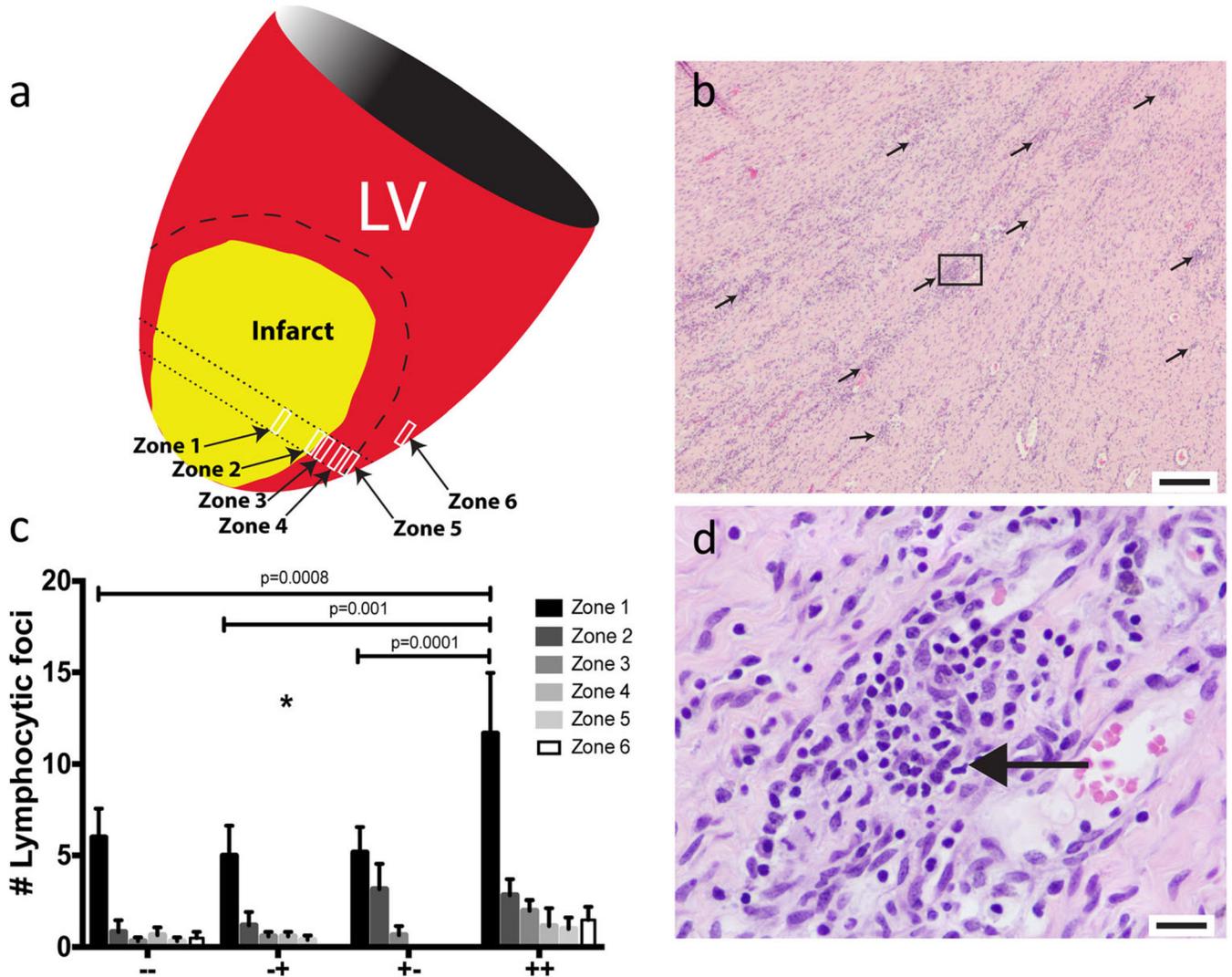
Fig. 6.
a Systematic histology assessment, sampled from six zones spanning from the infarct (zone 1), radiating outwardly across the border zone (zones 2– 5), and the unaffected interventricular septum (zone 6). **b** Representative 4× image of diffuse lymphocytic foci (*black arrows*) in the ++ treated group (scale bar=200 mm). **c** Average number of lymphocytic foci in each group per zone. There was a significant increase in lymphocytic foci in the ++ group compared to the other groups (p= 0.002) with the greatest difference in the infarct zone (zone 1). **d** High power (40×) image of the lymphocytic foci in the box in panel B, the *small round deeply purple nuclei* are lymphocytes (scale bar=20 mm)